QR-10120-02
December, 1989

Quarterly Progress Report for:
RADIATION-HARD HIGH-EFFICIENCY InP SPACE SOLAR CELL DEVELOPMENT

Covering the Period:
12 August 1989 to 11 November 1989

Submitted Under:
Contract N00014-89-C-2148

Submitted to:
NAVAL RESEARCH LABORATORY
4555 Overlook Avenue SW
Washington, DC 20375-5000

Submitted by:
SPIRE CORPORATION
Patriots Park
Bedford, MA 01730

1.0 SUMMARY

This quarter was marked by two serious problems which have delayed fabrication and delivery of the cells. The first of these problems, the failure of the front contact metallization, was solved in early November. The second problem, the abnormally low open-circuit voltages and fill factors, was not solved as of the end of the quarter, although promising indications have been seen in the interval between the end of the reporting period and this writing.

Despite these problems, we were able to continue work on the emitter structures; advanced thin emitters have been grown without any post-growth thinning step and have demonstrated improved quantum efficiency.

Development of the processing sequence has continued as well; details of the back contact formation process have been elucidated in order to give maximum flexibility for the processing of thin cells.

2.0 MOCVD CELL GROWTH

Growth has continued at atmospheric pressure; although low-pressure capability is available again, atmospheric pressure growth is more reliable and there is no indication that the improvements in uniformity available with low-pressure growth are significant for solar cell applications. Because of the delays in processing the cells, only four cell runs, a total of eight wafers, were completed; most of the experiments used material which was grown during the first quarter. (There were 13 calibration runs of various types.)

2.1 Advanced Emitter Structures

Experiments aimed at an improvement in the cell structure were made during this period. Previously, the emitters of these cells were formed by growing an n-type layer of 100 nm thickness, doped to 3×10^{18} cm^{-3}. These emitters were thinned during processing to about 20 nm thickness. Theoretical modeling and earlier experience with implanted cells has indicated that a heavier doping level at the surface could improve the cell performance, and the process could clearly be made more cost-effective and reliable if the thinning step could be eliminated.

With this end in view, a series of modified emitter structures was grown. First, the growth rate for the emitter portion of the cell was reduced from 1.1 nm/sec to approximately 0.15, to allow better control of the doping profile. Then, a series of runs at approximately the same doping concentration but different emitter growth times was made, to observe the relation between growth time, emitter thickness, and sheet conductivity. After this was done, the three emitter structures described in Figure 1 were grown, along with a control wafer. These wafers were processed into cells and tested; the results, which are given in another section below, show that the two-step emitter structure yields a significantly higher short-circuit current and blue response than the control.

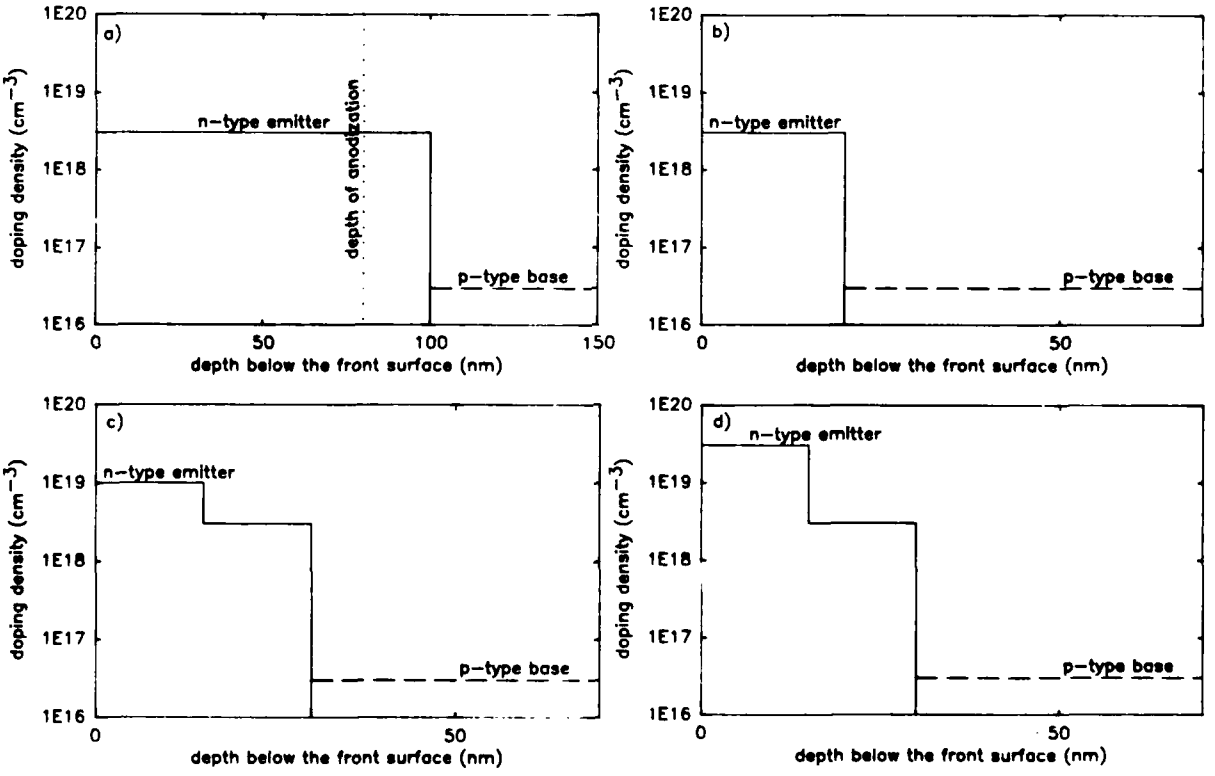

FIGURE 1. EMITTER STRUCTURES GROWN DURING THIS PERIOD. a) Standard emitter structure. The emitter is grown 100 nm thick and then etched to 20 nm. b) One-step thin emitter. A slower growth rate is used, and the emitter is grown to 20 nm thickness, eliminating the need for etching. c) and d) Two-step thin emitters. The higher doping near the surface creates a field which improves the collection of carriers.

These structures were characterized by differential Hall effect measurements; the results for one run are shown in Table 1. Although there is considerable scatter in the data due to the small thicknesses involved, the results indicate that the actual doping profile in the emitter is acceptably close to the desired one.

TABLE 1. DIFFERENTIAL HALL MEASUREMENT OF RUN NO. 905.

Step #	Depth (nm)	Dopant Concentration (cm^{-3})
1	0–6	1.3×10^{19}
2	6–11	2.7×10^{19}
3	11–17	7.0×10^{18}
4	17–23	4.8×10^{18}

2.2 Cap layers

According to plan, the processes for growing InGaAs cap layers are being developed. The first cell structure with an InGaAs cap layer was grown during this period. X-ray fluorescence measurements show that the material is within a few percent of the correct composition (Figure 2), but cell results were not available during this reporting period. Work on the uniformity of the InGaAs is continuing, although for use as a cap layer, an exact lattice match may not be necessary.

3.0 CELL PROCESSING

3.1 Front Contact Formation

Two unforeseen technical problems concerning the front contact formation arose in September. The first of these manifested itself as a separation of the metallization from the InP during the front contact sinter; gas bubbles appeared under the metal in some places, and adhesion of the metal afterward was essentially nil, although the wafers would pass the tape test before sintering. We had never previously observed this phenomenon. By means of a series of experiments, contamination of the evaporation chamber and of the evaporation source was eliminated. It was found that InP wafers without photoresist did not suffer from this problem. Therefore, although silicon test wafers were not affected, it was concluded that contamination on the surface of the wafer was responsible. A number of cleaning procedures were tested in attempts to remove this hypothetical contamination,

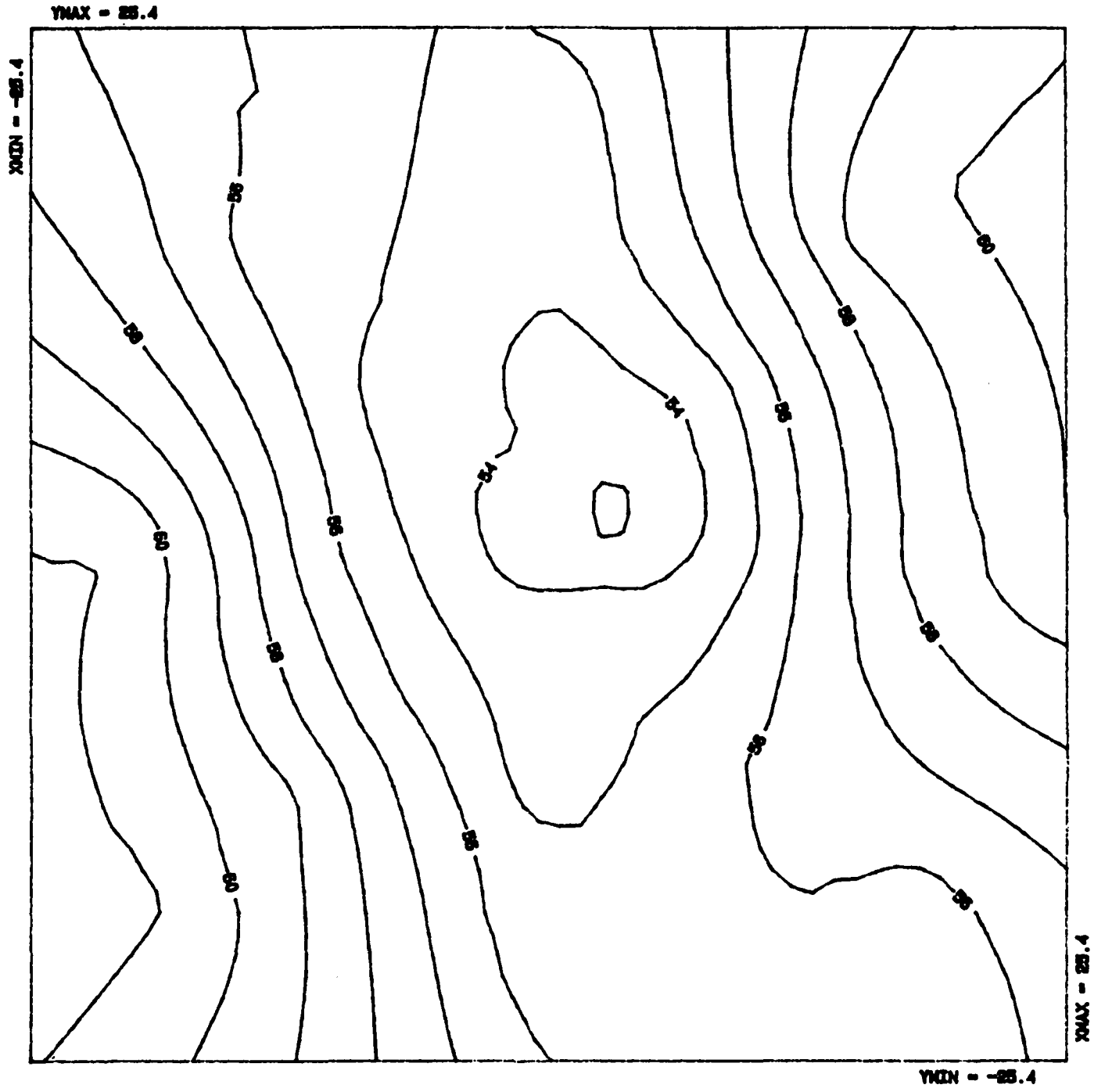

M05-967 Indium Fraction

FIGURE 2. COMPOSITION OF AN InGaAs LAYER GROWN ON InP. The indium fraction (x) increases toward the sides of the wafer, but the small lattice match introduced (0.3%) may be acceptable for the purposes of a cap layer.

and one was found to be successful: exposure to oxygen plasma. In two cases, cleaned and uncleaned wafers were processed together, and the uncleaned wafers failed while the cleaned wafers showed no failure. The separation during the sinter has not recurred since the oxygen plasma was made a part of the process.

The second problem, which arose immediately after the first problem was solved, involved the separation of the metallization from the InP before the sinter, during the liftoff process. Typically, most of the grid lines and pads would come off of the wafer, and those that remained would be easily removed by the tape test.

Contamination was again suspected, but another thorough cleaning of the equipment and a set of experiments with different procedures yielded no positive results. Substituting Ti-Pd-Ag layers for the Cr-Au-Ag produced no change. In an attempt to drive off water vapor or other volatile substances from the surface, we increased the wafer temperature to 90°C during the evaporation; this gave no improvement.

We found that thin layers (less an 0.5 micron) did not suffer from this poor adhesion; it arose only when larger amounts of silver were used. This led to the hypothesis that stress in the silver film was responsible for the failure. Accordingly, we added water cooling during the evaporation to keep the wafer temperature closer to room temperature (previously it had been allowed to rise with the heat from the evaporation to approximately 60°C). This was successful: the adhesion returned and has not failed since that point.

3.2 Back Contact Formation

Meanwhile, work continued on the back contact metallurgy. The film described in the last report was investigated further and found to be a zinc-phosphorus compound, which evaporates from the film when it is alloyed at low pressure, but remains on the wafer if the alloying is done at atmospheric pressure.

The behavior of the film was investigated as a function of both zinc content and alloying temperature. It was found that reducing the zinc content from 25% to 5 or 10% reduced the evolution of this volatile compound.

The film was seen to pass through three distinct stages, distinguishable by the naked eye during the alloying process. First, a light reddish color replaces the gold;

according to Fatemi,[1] this indicates the formation of Au_3In. Second, the film becomes colorless again, with the formation of $AuIn_2$. Finally, when the eutectic point is reached and the film becomes liquid, it appears more reflective and patterns of crystallization are visible after cooling.

These data will be useful in the effort to make thinner cells, since it may be necessary to form the back contact after the front contact, and this may require a reduced heat treatment.

3.3 Process Yield

The high breakage experienced with the first lot of 2 x 2 cells has not been repeated. With additional practice in handling the InP wafers, the physical yield has improved to approximately 75%, based on the most recent lots.

4.0 CELL RESULTS

4.1 Baseline Cells

Table 2 shows the measurement results of the baseline cells fabricated in this period. After antireflection coating, two of the cells meet the efficiency goal of 15% for the first group of deliverable cells; the remainder show a very wide variation.

This variation shows that there is some unknown variable affecting the cell performance, which is responsible for the low V_{oc} and fill factor of most of the cells. As before, the shape of the I-V curves indicates that the problem is in the space-charge region.

4.2 Advanced Emitter Growth

Cells were made from the advanced emitters described in section 1. Table 3 gives the results by category.

These measurements were made under a simulated AM0 spectrum at 25°C. Currents were corrected for the spectral mismatch between the InP cell and the GaAs reference cell. Current densities and efficiencies were calculated on a total area basis, using a value of 137.2 mW/cm^2 for the solar constant.

TABLE 2. PERFORMANCE OF THE BASELINE CELLS.

Cell #	Area (cm^2)	Open-circuit Voltage (V)	Short-circuit Current (mA/cm^2)	Fill Factor (%)	Eff.
			Lot 5266		
7-2	4.00	0.651	21.62	64.4	6.6[a]
5-2	4.00	0.845	22.36	81.3	11.2[a]
3-2	4.00	0.804	22.42	68.1	8.9[a]
2-2	4.00	0.808	20.14	68.6	8.1[a]
6-2	4.00	0.814	20.95	77.6	9.6[a]
4L-2	4.00	0.780	18.90	69.5	7.5[a]
4R-2	4.00	0.811	17.08	74.1	7.5[ab]
			Lot 5269		
3-1	4.00	0.798	22.96	77.4	10.3[a]
1L-2	4.00	0.836	28.99	78.8	13.9[ac]
1R-2	4.00	0.836	28.41	78.9	13.7[ac]
2-1	4.00	0.592	22.61	39.2	3.8[a]
2-2	4.00	0.805	22.50	69.6	9.2[a]
4-1	4.00	0.732	22.32	69.2	8.2[a]
4-2	4.00	0.722	22.62	73.9	8.8[a]
5-1	4.00	0.734	22.34	75.6	9.0
5-2	4.00	0.732	22.68	75.1	9.1
			Lot 5281		
7-1	4.00	0.803	22.87	74.2	9.9
7-2	4.00	0.792	22.87	73.2	9.7
8-2	4.00	0.774	22.97	72.5	9.4
8-1	4.00	0.761	17.83	71.0	7.0
2-1	4.00	0.746	22.29	70.1	8.5
2-2	4.00	0.764	21.89	77.0	9.4
1-1	4.00	0.794	20.61	76.2	9.1
1-2	4.00	0.791	20.66	74.4	8.9
3-1	4.00	0.834	22.65	77.2	10.6
3-2	4.00	0.818	22.54	76.1	10.2

Notes:

a These cells suffered from poor metal adhesion. The problem was subsequently corrected by using an O_2 plasma clean before evaporation.

b This wafer has a lower-than-normal J_{SC} because it was processed without anodizing, as a control.

c This wafer has a higher-than-normal J_{SC} because it has a layer of SiO_2, which acts as a partial antireflection coating.

TABLE 3. LOT 5271. (Study of thin MOCVD-grown emitters)

Cell #	Area (cm^2)	Open-circuit Voltage (V)	Short-circuit Current (mA/cm^2)	Fill Factor (%)	Eff.	Internal QE 400 nm
			Control Group (anodized emitter)			
1-2	4.00	0.679	22.61	77.8	8.7	
2-1	1.00	0.760	21.86	76.9	9.3	
2-2	1.00	0.749	21.51	75.1	8.8	
2-3	1.00	0.791	20.61	77.4	9.2	
			Run # 899 (one-step emitter)			
3-1	1.00	0.772	21.03	49.4	5.8	0.339
3-2	1.00	0.748	20.83	32.7	3.7	
3-3	1.00	0.781	21.07	49.3	5.9	
4-2	4.00	0.720	21.65	76.0	8.6	0.341
			Run # 904 (two-step emitter)			
6-2	4.00	0.731	22.89	78.2	9.5	0.476
			Run # 905 (two-step emitter)			
7-1	4.00	0.694	23.94	78.9	9.6	0.564
7-2	4.00	0.689	23.85	78.7	9.4	
8-1	1.00	0.758	23.65	79.7	10.4	
8-2	1.00	0.780	23.54	80.2	10.7	0.565
8-3	1.00	0.787	23.56	80.0	10.8	
8-4	1.00	0.732	19.69	44.6	4.7	
8-5	1.00	0.764	23.60	79.8	10.5	
8-6	1.00	0.771	23.85	78.2	10.5	
8-7	0.25	0.751	22.89	78.3	9.8	
8-8	0.25	0.748	22.92	79.4	9.9	
8-11	0.25	0.747	24.10	75.9	10.0	
8-12	0.25	0.752	23.28	79.0	10.1	0.555
8-13	0.25	0.738	22.65	1.7	0.2	
8-14	0.25	0.735	23.69	73.6	9.3	
8-16	0.25	0.738	22.84	78.5	9.7	

For comparison, the internal quantum efficiencies of the baseline cells made so far have been in the range of 0.35 to 0.45 at 400 nm, so the two-step emitter represents a definite improvement. The corresponding parameter from the 18.8% efficient epitaxial/implanted cell was 0.67.

5.0 DISCUSSION OF RESULTS

Various hypotheses were considered for the cause of the low voltages and fill factors. Since the emitters of the cells are very thin, the space-charge region is close to the surface, and some sort of damage to the surface during processing is the most obvious explanation of our results. Accordingly, the cell performance was examined with respect to the following processing variables:

5.1 Emitter Thickness

Since there is a considerable variability in the anodization process, the actual emitter thickness is not constant. Assuming a constant resistivity for the emitter material, however, the actual emitter thickness can be measured on each wafer by measuring the sheet resistance. Figure 3 is a scatter plot of the measured emitter thickness against the open-circuit voltage of the cells. It is clear from the figure that the correlation is uncertain, that most of the variation must be accounted for by some other variable.

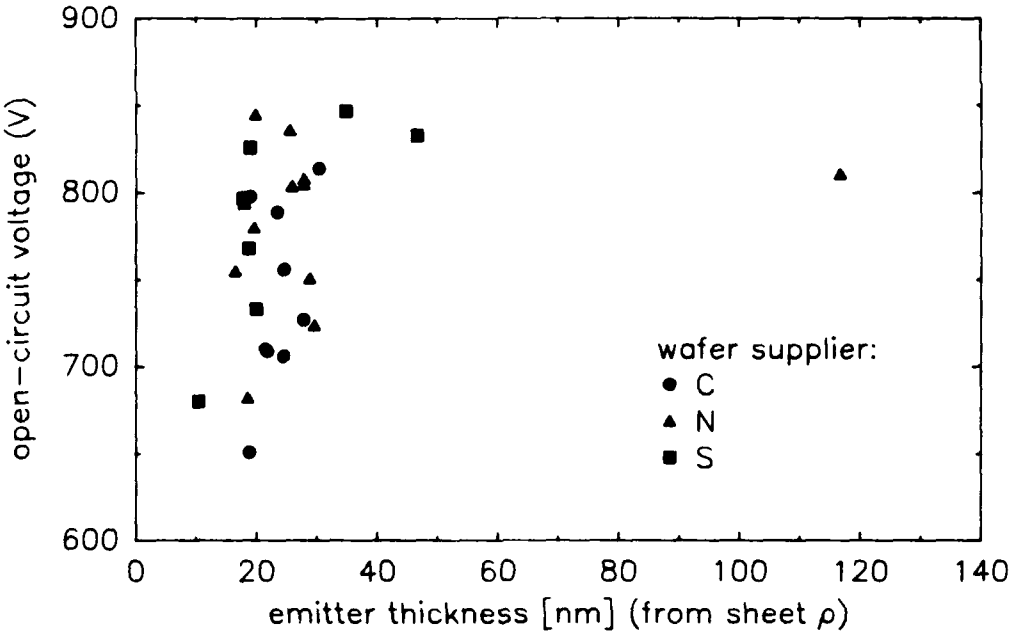

FIGURE 3. SCATTER PLOT OF CELL OPEN-CIRCUIT VOLTAGE AGAINST EMITTER THICKNESS. The data indicate a very weak correlation; there is apparently another variable which degrades the cell performance.

5.2 Substrate Source

A similar attempt was made to correlate the cell performance with the substrate manufacturer. Again, the correlation was uncertain, and great variations occurred within a single substrate batch.

5.3 Base Doping Level

Although the quantum efficiency measurements indicate that the carrier lifetime in the base is good, an indirect effect of the base doping concentration is possible. Since the base doping level influences the width of the space-charge region, a lower base doping may lead to greater recombination in the space-charge region and therefore lower voltage. This is considered a possibility since the base doping of the cells reported here is somewhat lower than that of the successful cells made earlier (10^{16} cm^{-3} instead of 3 x 10^{16} cm^{-3}).

5.4 Back Contact Anneal

Another possibility is the variation in temperature of the back contact anneal. The furnace in which the anneal is done shows considerable variation from point to point; this can be observed by means of the color changes which the back contact undergoes. (See the previous section.) Preliminary results show that the best cells were among the ones which were heated to the lowest temperature, but there is not enough data at this point to be conclusive.

5.5 Cap Layers

Although we know it is possible to make good cells with the simple shallow-homojunction structure which we have been using, it may be possible to do so more reliably by adding a low-bandgap cap layer between the emitter and the front metal contacts. This is a step which we have planned to incorporate into the process for various reasons since the beginning of the project, and, from the nature of the current problem, it appears as though it may be helpful in protecting the surface during processing.

6.0 CURRENT PLANS

The course of action for the coming quarter is clear. First, the cause of the low voltages and fill factors must be identified and corrected. Experiments will be carried out to this end in the three areas discussed above: addition of InGaAs cap layers, increase in

the base doping density, and modification of the back contact anneal step. When we are satisfied that the cell fabrication process is reliable, we will fabricate the deliverable cells which are past due.

Concurrently, we will continue with the planned program of further cell development, which includes further development of advanced emitter structures, cap layers, contact testing, and radiation testing, to the extent that it will not delay the cell fabrication.

7.0 REFERENCE

1. N.S. Fatemi and V.G. Weizer, "Semiconductor structural damage attendant to contact formation in III-V solar cells," Tenth NASA Space Photovoltaic Research and Development Conference, Cleveland, November 1989.

APPENDIX A
DETAILED CELL DATA

This appendix contains performance data for all cells made during this period (Table A-1), I-V curves for ten selected cells, and quantum efficiency curves for five selected cells (attached).

TABLE A-1. PERFORMANCE OF THE BASELINE CELLS.

Cell #	Area (cm^2)	Open-circuit Voltage (V)	Short-circuit Current (mA/cm^2)	Maximum Power (mW)	Fill Factor	Eff. (%)
			Lot 5266 (27 Sept 89)			
7-2	4.00	0.651	21.62	36.23	64.4	6.6
7-4	0.25	0.555	16.46	1.28	55.8	3.7
7-5	0.25	0.361	18.77	1.04	61.3	3.0
5-2	4.00	0.845	22.36	61.44	81.3	11.2
5-4	0.25	0.823	22.19	3.13	68.6	9.1
5-5	0.25	0.838	20.12	3.37	79.9	9.8
3-2	4.00	0.804	22.42	49.11	68.1	8.9
3-4	0.25	0.513	22.02	1.80	63.8	5.2
3-5	0.25	0.454	22.09	1.70	67.8	5.0
2-2	4.00	0.808	20.14	44.69	68.6	8.1
2-4	0.25	0.810	22.79	3.27	71.0	9.5
2-5	0.25	0.804	23.13	3.43	73.7	10.0
6-2	4.00	0.814	20.95	52.92	77.6	9.6
6-4	0.25	0.769	20.49	2.92	74.1	8.5
4L-4	0.25	0.717	22.50	2.81	69.7	8.2
4L-2	4.00	0.780	18.90	41.02	69.5	7.5
4R-2	4.00	0.811	17.08	41.05	74.1	7.5
1-4	0.25	0.701	22.00	2.50	64.8	7.3
			Lot 5266 after AR (16 Nov 89)			
5-2	4.00	0.857	32.19	88.07	79.8	16.1
6-2	4.00	0.828	30.28	75.06	74.9	13.7
			Lot 5269			
3-1	4.00	0.798	22.96	56.74	77.4	10.3
3-5	0.25	0.812	21.76	3.37	76.3	9.8
3-4	0.25	0.571	16.55	1.45	61.3	4.2
1L-2	4.00	0.836	28.99	76.43	78.8	13.9
1R-2	4.00	0.836	28.41	74.96	78.9	13.7
2-1	4.00	0.592	22.61	20.97	39.2	3.8
2-2	4.00	0.805	22.50	50.45	69.6	9.2
4-1	4.00	0.732	22.32	45.24	69.2	8.2
4-2	4.00	0.722	22.62	48.31	73.9	8.8
5-1	4.00	0.734	22.34	49.51	75.6	9.0
5-2	4.00	0.732	22.68	49.86	75.1	9.1
5-4	0.25	0.631	22.63	2.32	64.9	6.8
5-5	0.25	0.774	20.91	3.23	79.9	9.4
4-4	0.25	0.584	4.72	0.28	41.2	0.8

TABLE A-1. PERFORMANCE OF THE BASELINE CELLS. (Continued)

Cell #	Area (cm^2)	Open-circuit Voltage (V)	Short-circuit Current (mA/cm^2)	Maximum Power (mW)	Fill Factor	Eff. (%)
			Lot 5269 after AR (16 Nov 89)			
1-2	4.000	0.838	31.15	81.87	78.4	14.9
2-2	4.000	0.820	32.86	74.75	69.3	13.6
2-1	4.000	0.827	32.74	72.47	66.9	13.2
5-1	4.000	0.750	32.76	73.27	74.5	13.4
5-2	4.000	0.748	33.00	72.83	73.9	13.3
3-1	4.000	0.770	32.41	74.91	75.1	13.7
			Lot 5271 (16 Nov 89)			
4-2	4.000	0.720	21.65	47.44	76.0	8.6
1-2	4.000	0.679	22.61	47.78	77.8	8.7
7-1	4.000	0.694	23.94	52.43	78.9	9.6
7-2	4.000	0.689	23.85	51.67	78.7	9.4
6-2	4.000	0.731	22.89	52.35	78.2	9.5
3-1	1.000	0.772	21.03	8.03	49.4	5.8
3-2	1.000	0.748	20.83	5.10	32.7	3.7
3-3	1.000	0.781	21.07	8.11	49.3	5.9
2-1	1.000	0.760	21.86	12.77	76.9	9.3
2-2	1.000	0.749	21.51	12.10	75.1	8.8
2-3	1.000	0.791	20.61	12.61	77.4	9.2
8-1	1.000	0.758	23.65	14.29	79.7	10.4
8-2	1.000	0.780	23.54	14.73	80.2	10.7
8-3	1.000	0.787	23.56	14.82	80.0	10.8
8-4	1.000	0.732	19.69	6.43	44.6	4.7
8-5	1.000	0.764	23.60	14.39	79.8	10.5
8-6	1.000	0.771	23.85	14.36	78.2	10.5
8-7	0.250	0.751	22.89	3.36	78.3	9.8
8-8	0.250	0.748	22.92	3.40	79.4	9.9
8-11	0.250	0.747	24.10	3.42	75.9	10.0
8-12	0.250	0.752	23.28	3.46	79.0	10.1
8-13	0.250	0.738	22.65	0.07	1.7	0.2
8-14	0.250	0.735	23.69	3.20	73.6	9.3
8-16	0.250	0.738	22.84	3.31	78.5	9.7
			Lot 5281 (14 Nov 89)			
7-1	4.00	0.803	22.87	54.50	74.2	9.9
7-2	4.00	0.792	22.87	53.04	73.2	9.7
8-2	4.00	0.774	22.97	51.51	72.5	9.4
8-1	4.00	0.761	17.83	38.54	71.0	7.0
2-1	4.00	0.746	22.29	46.61	70.1	8.5
2-2	4.00	0.764	21.89	51.51	77.0	9.4
1-1	4.00	0.794	20.61	49.87	76.2	9.1
1-5	0.25	0.803	19.54	3.06	78.0	8.9
1-2	4.00	0.791	20.66	48.64	74.4	8.9
3-1	4.00	0.834	22.65	58.32	77.2	10.6
3-5	0.25	0.851	21.53	3.69	80.6	10.8
3-2	4.00	0.818	22.54	56.09	76.1	10.2

TABLE A-1. PERFORMANCE OF THE BASELINE CELLS. (Concluded)

Cell #	Area (cm^2)	Open-circuit Voltage (V)	Short-circuit Current (mA/cm^2)	Maximum Power (mW)	Fill Factor	Eff. (%)
			Lot 5281 after AR (16 Nov 89)			
6-1	4.00	0.778	30.61	66.55	69.9	12.1
2-1	4.00	0.763	32.02	70.89	72.5	12.9
2-2	4.00	0.781	31.93	75.76	75.9	13.8
8-2	4.00	0.786	32.88	74.16	71.7	13.5
8-1	4.00	0.776	25.45	55.51	70.3	10.1
3-1	4.00	0.846	32.25	82.75	75.8	15.1
3-2	4.00	0.830	32.51	80.73	74.8	14.7

These measurements were made under a simulated AM0 spectrum at 25°C. Currents were corrected for the spectral mismatch between the InP cell and the GaAs reference cell. Current densities and efficiencies were calculated on a total area basis, using a value of 137.2 mW/cm^2 for the solar constant.

Sample ID: 5271-2-2
QE File: B:527122S.QE 01-03-1990 15:11:30 Shadow: .035
Ref File: B:527122S.REF 01-03-1990 15:11:30

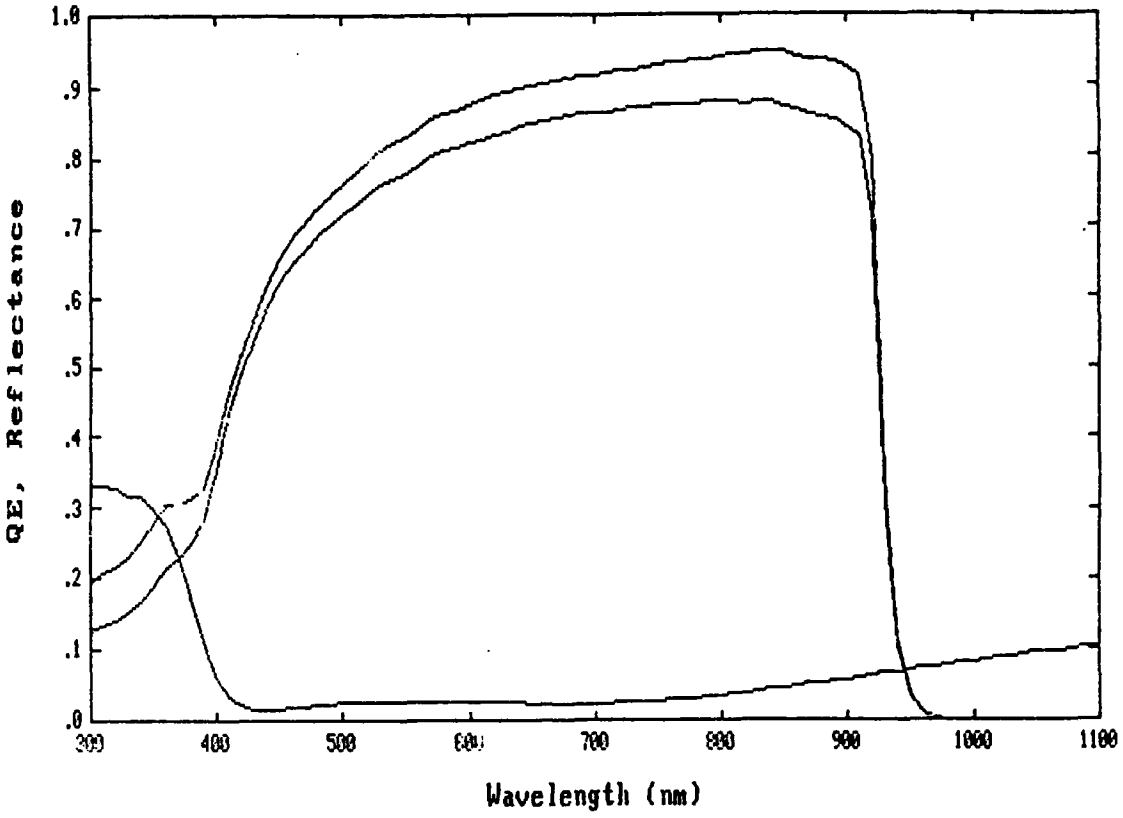

Sample ID: 5271-7-1
QE File: B:5271-7-1.QE 11-21-1989 16:15:17 Shadow: .000
Ref File: B:5271-7-1.REF 11-21-1989 16:15:17

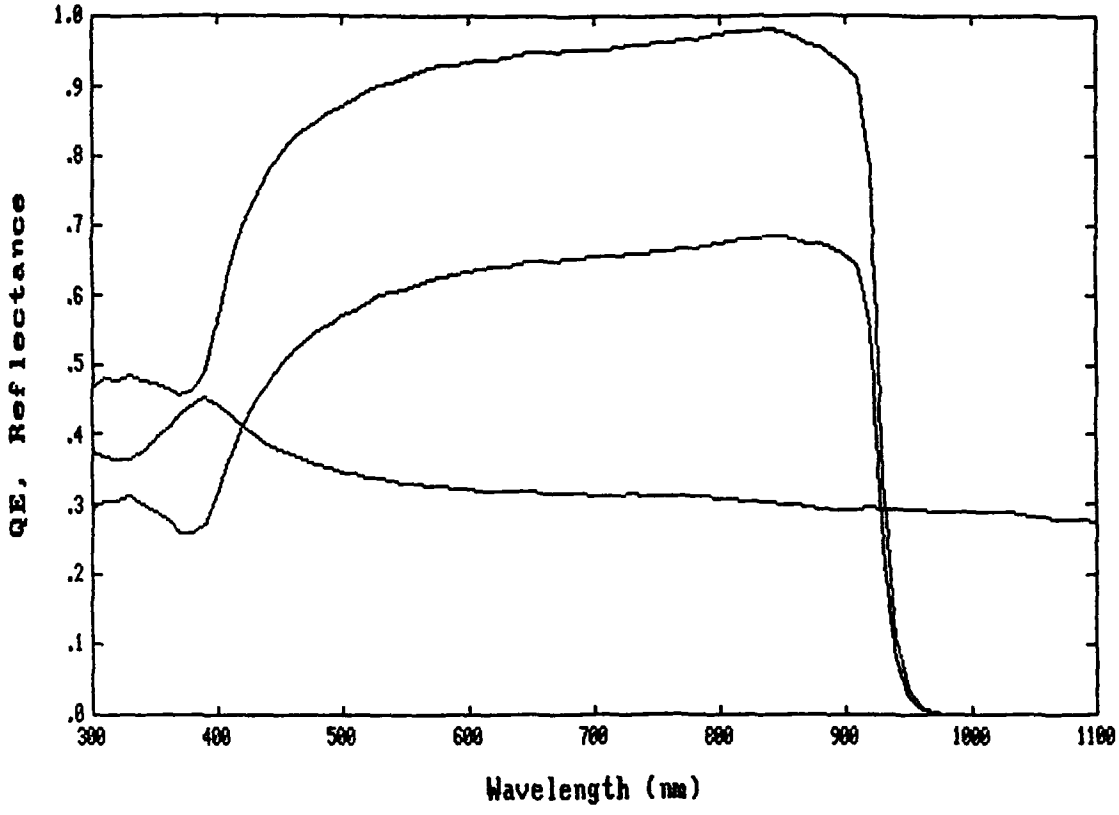

Sample ID: 5271-7-1
QE File: B:527171S.QE 01-03-1990 14:53:01 Shadow: .035
Ref File: B:527171S.REF 01-03-1990 14:53:01

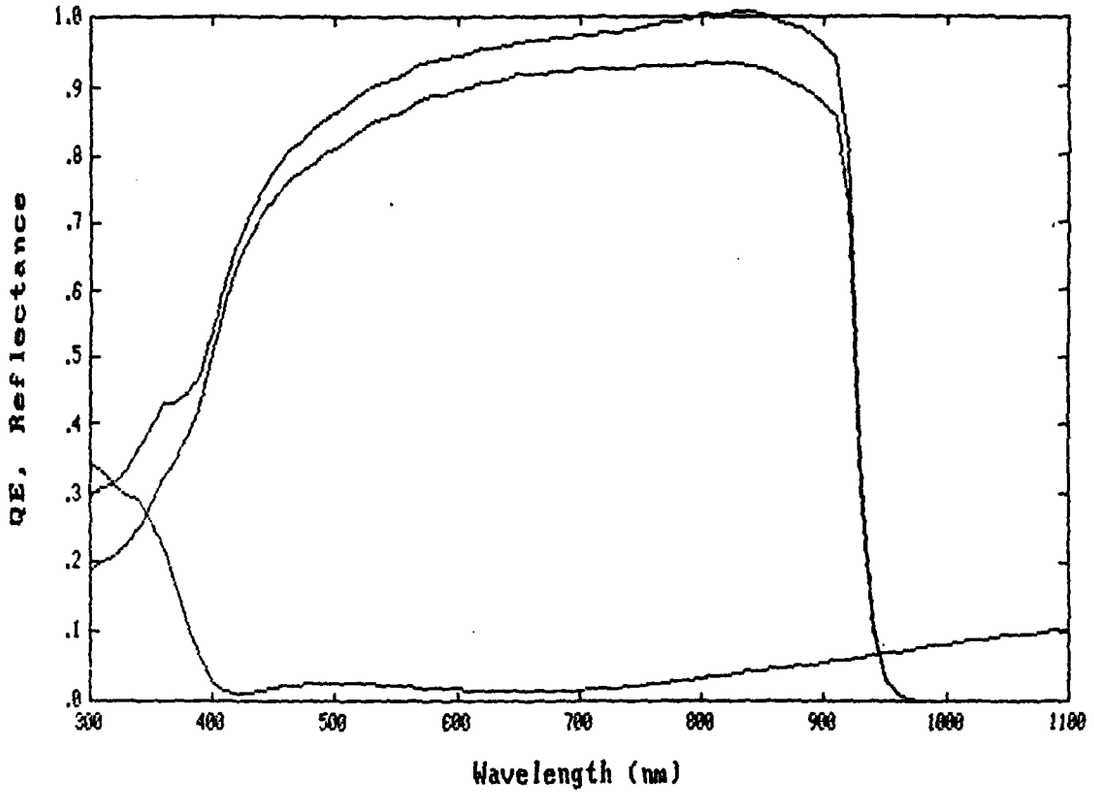

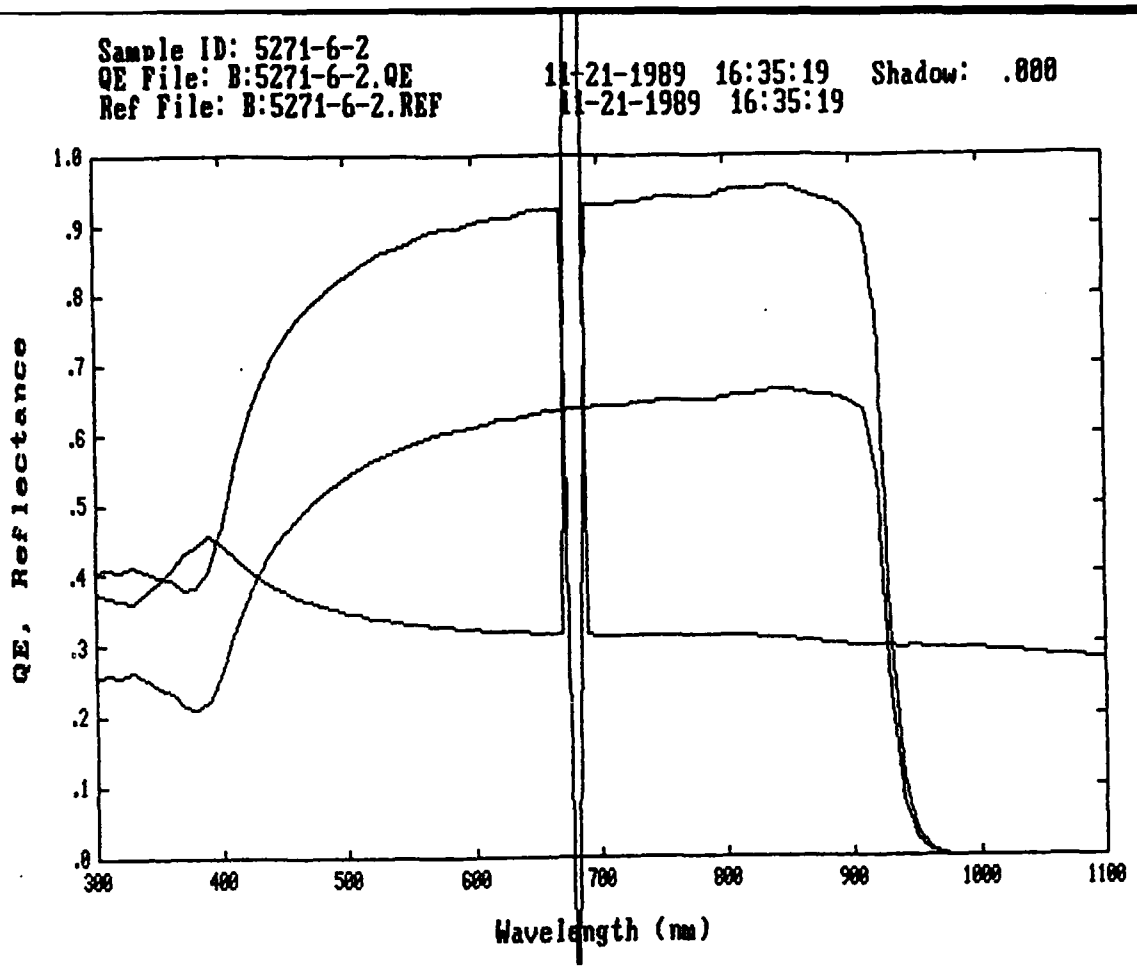
Sample ID: 5271-6-2
QE File: B:5271-6-2.QE
Ref File: B:5271-6-2.REF
11-21-1989 16:35:19
11-21-1989 16:35:19
Shadow: .000
QE, Reflectance
1.0
.9
.8
.7
.6
.5
.4
.3
.2
.1
.0
300
400
500
600
700
800
900
1000
1100
Wavelength (nm)

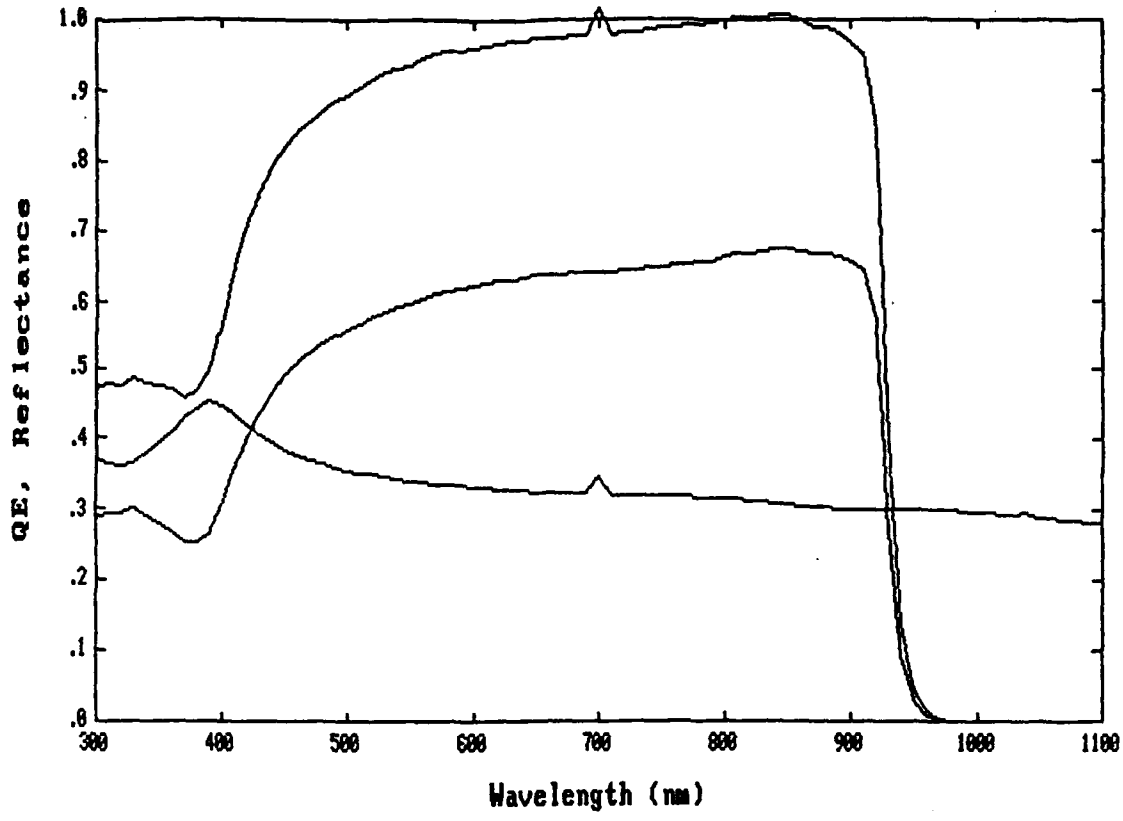
Sample ID: 5271-8-2
QE File: B:527182QE.QE 11-27-1989 13:26:09 Shadow: .035
Ref File: B:527182QE.REF 11-27-1989 13:26:09
QE, Reflectance
1.0
.9
.8
.7
.6
.5
.4
.3
.2
.1
.0
300
400
500
600
700
800
900
1000
1100
Wavelength (nm)

Sample ID: 5271-4-2
QE File: B:527142.QE 11-21-1989 15:51:18 Shadow: .000
Ref File: B:527142.REF 11-21-1989 15:51:18

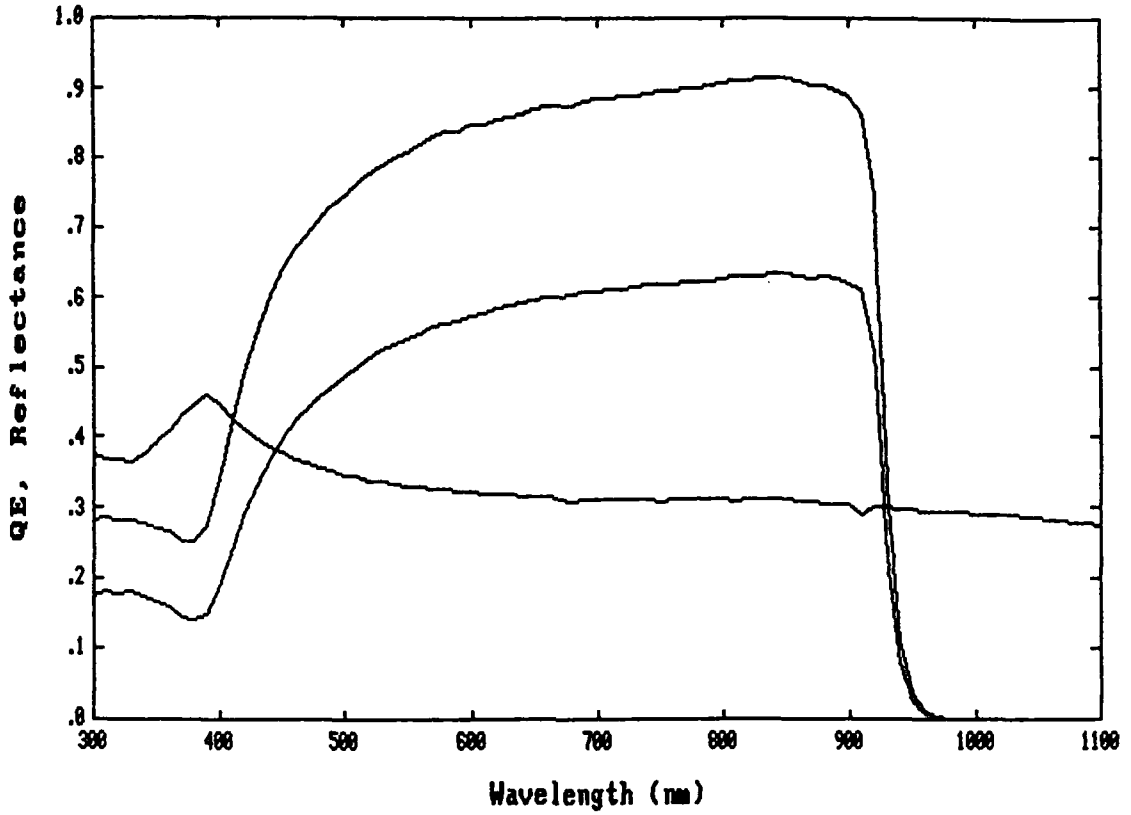

Lot: 5266-1 Contract: 10120
Material: InP/Si AR Coat: None
Surface: Specular Temp: 25C
Ref. Cell: ST419 Ref Isc: 8.2 mA
Comment: RESIST STRIPPED
Spectrum: AM0 (137.2 mW/cm2)
V Chan.: 3 I Chan.: 4 Cell Type: Sm. n/p

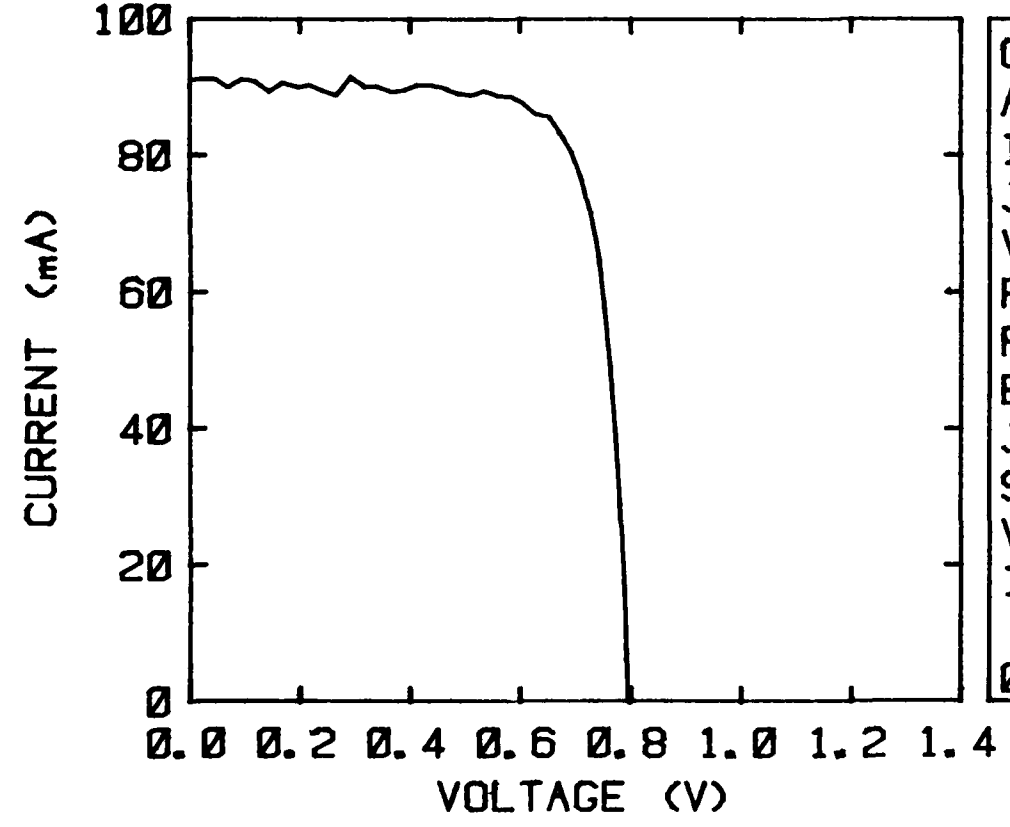

Cell 31		
Area	4.000	cm2
Isc	90.465	mA
Jsc	22.62	mA/cm2
Voc	0.798	V
Pmax	55.889	mW
FF	77.41	%
Eff	10.18	%
Jsc1	22.62	mA/cm2
Suns	1.0	
Vm	0.671	V
Im	83.265	mA

09-26-1989 13:45:50

Lot: 5266-1
Material: InP/Si
Surface: Specular
Ref. Cell: ST419
Comment: RESIST STRIPPED
Spectrum: AM0 (137.2 mW/cm2)
V Chan.: 3
I Chan.: 4
Contract: 10120
AR Coat: None
Temp: 25C
Ref Isc: 8.2 mA
Cell Type: Sm. n/p

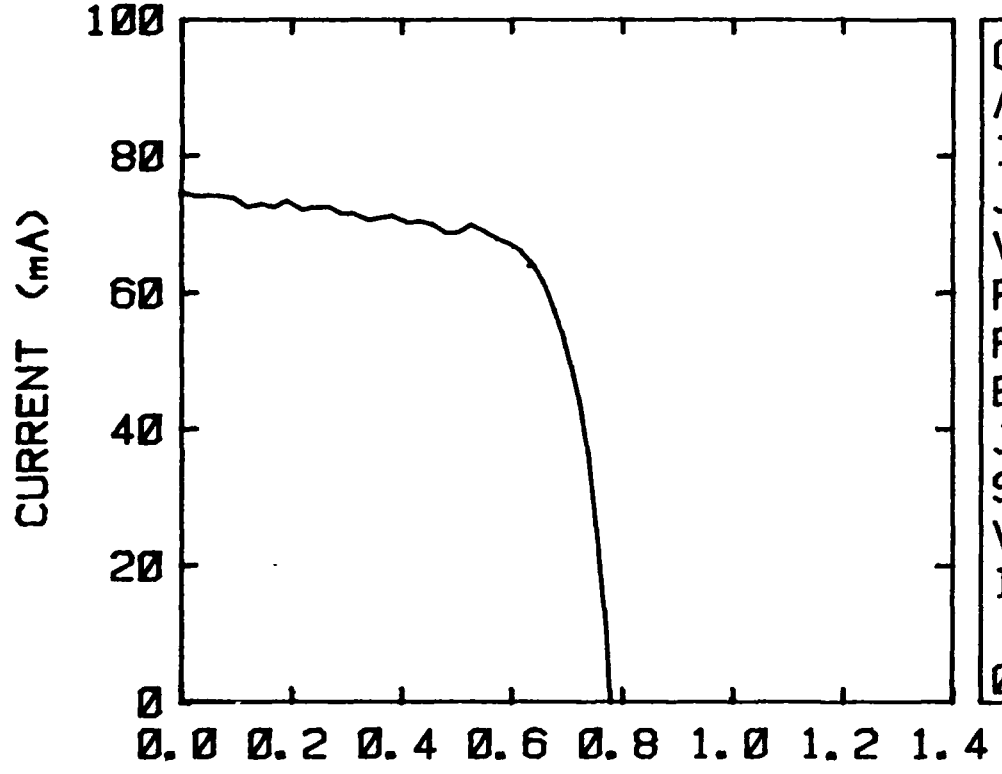

Cell 412		
Area	4.000	cm2
Isc	74.489	mA
Jsc	18.62	mA/cm2
Voc	0.780	V
Pmax	40.407	mW
FF	69.52	%
Eff	7.36	%
Jsc1	18.62	mA/cm2
Suns	1.0	
Vm	0.632	V
Im	63.892	mA

09-27-1989 11:20:51

Lot: 5266-1	Contract: 10120
Material: InP/Si	AR Coat: None
Surface: Specular	Temp: 25C
Ref. Cell: ST419	Ref Isc: 8.2 mA
Comment: RESIST STRIPPED	
Spectrum: AM0 (137.2 mW/cm2)	
V Chan.: 3	I Chan.: 4

Cell Type: Sm. n/p

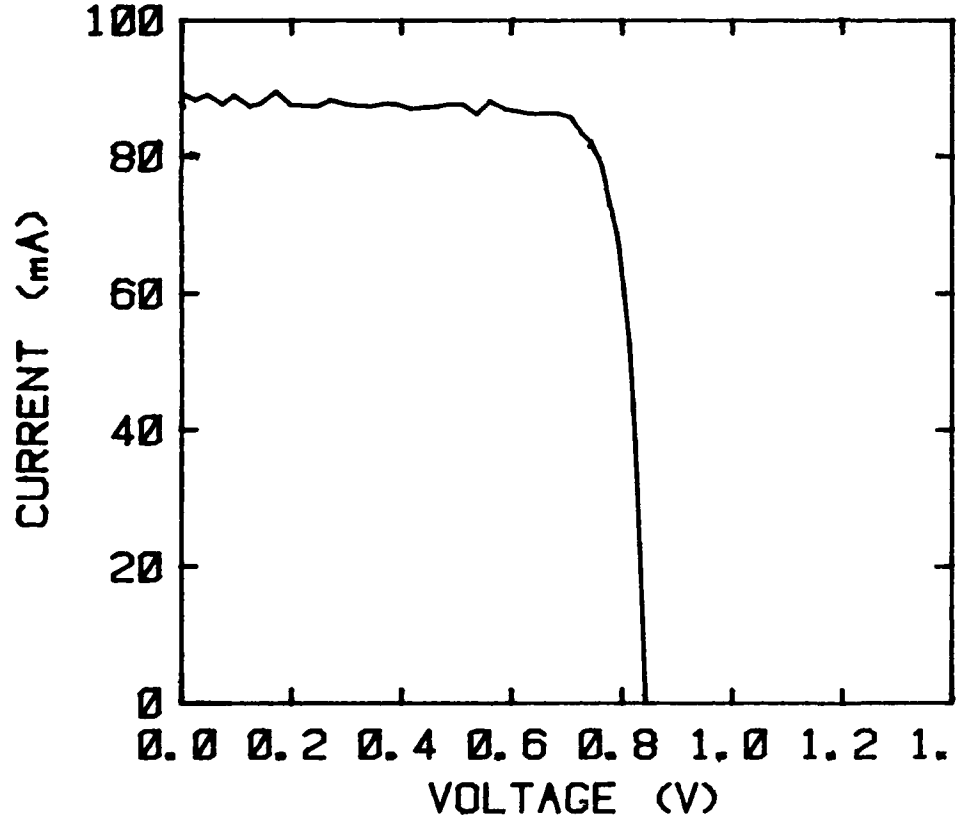

Cell 52		
Area	4.000	cm2
Isc	88.080	mA
Jsc	22.02	mA/cm2
Voc	0.845	V
Pmax	60.514	mW
FF	81.32	%
Eff	11.03	%
Jsc1	22.02	mA/cm2
Suns	1.0	
Vm	0.742	V
Im	81.529	mA

09-26-1989 14:21:50

Lot: 5269
Material: InP
Surface: Specular
Ref. Cell: ST17
Comment:
Spectrum: AM0 (137.2 mW/cm2)

Contract: 10120
AR Coat: MgF2/ZnS
Temp: 25C
Ref Isc: 8.1 mA

V Chan.: 3 I Chan.: 4 Cell Type: Sm. n/p

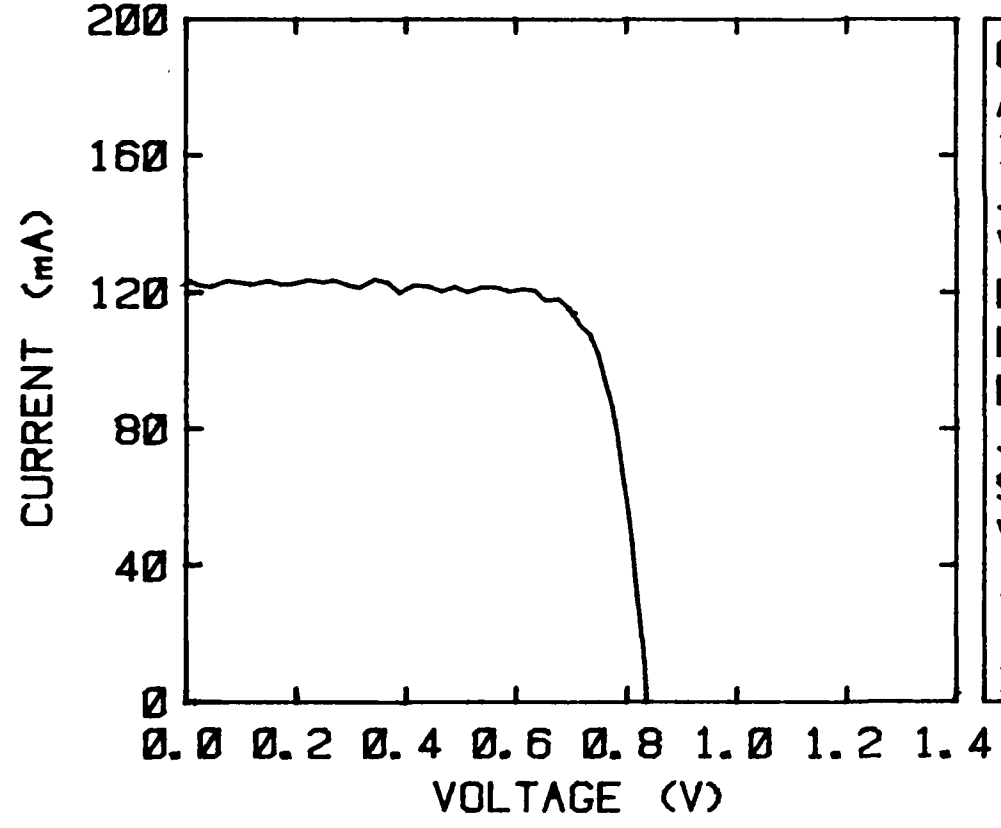

Cell 1-2		
Area	4.000	cm2
Isc	122.723	mA
Jsc	30.68	mA/cm2
Voc	0.838	V
Pmax	80.644	mW
FF	78.42	%
Eff	14.69	%
Jsc1	30.68	mA/cm2
Suns	1.0	
Vm	0.708	V
Im	113.908	mA

11-16-1989 14:55:55

Lot: 5269
Material: InP
Surface: Specular
Ref. Cell: ST17
Comment:
Spectrum: AM0 (137.2 mW/cm2)

Contract: 10120
AR Coat: MgF2/ZnS
Temp: 25C
Ref Isc: 8.1 mA

V Chan.: 3 I Chan.: 4 Cell Type: Sm. n/p

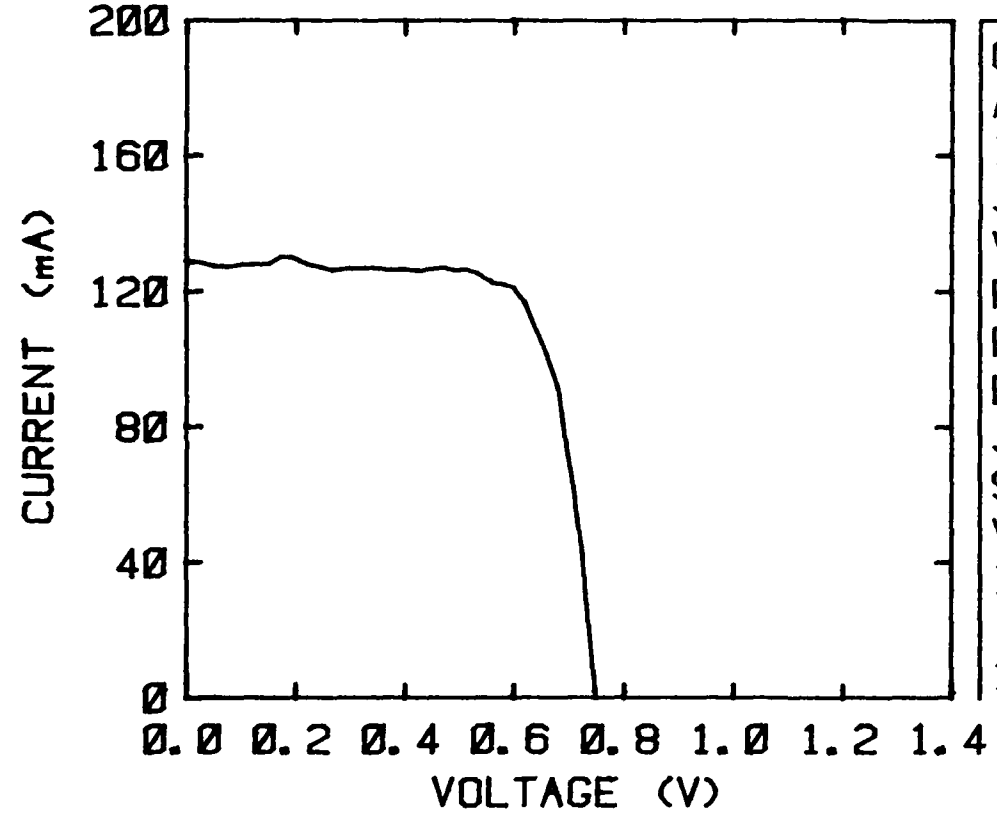

Cell 5-1		
Area	4.000	cm2
Isc	129.058	mA
Jsc	32.26	mA/cm2
Voc	0.750	V
Pmax	72.174	mW
FF	74.53	%
Eff	13.15	%
Jsc1	32.26	mA/cm2
Suns	1.0	
Vm	0.618	V
Im	116.725	mA

11-16-1989 15:04:29

Lot: 5281	Contract: 10120
Material: InP	AR Coat: None
Surface: Specular	Temp: 25C
Ref. Cell: ST17	Ref Isc: 8.1 mA

Comment: BEFORE FRONT CONTACT SINTER
Spectrum: AM0 (137.2 mW/cm2)
V Chan.: 3 I Chan.: 4 Cell Type: Sm. n/p

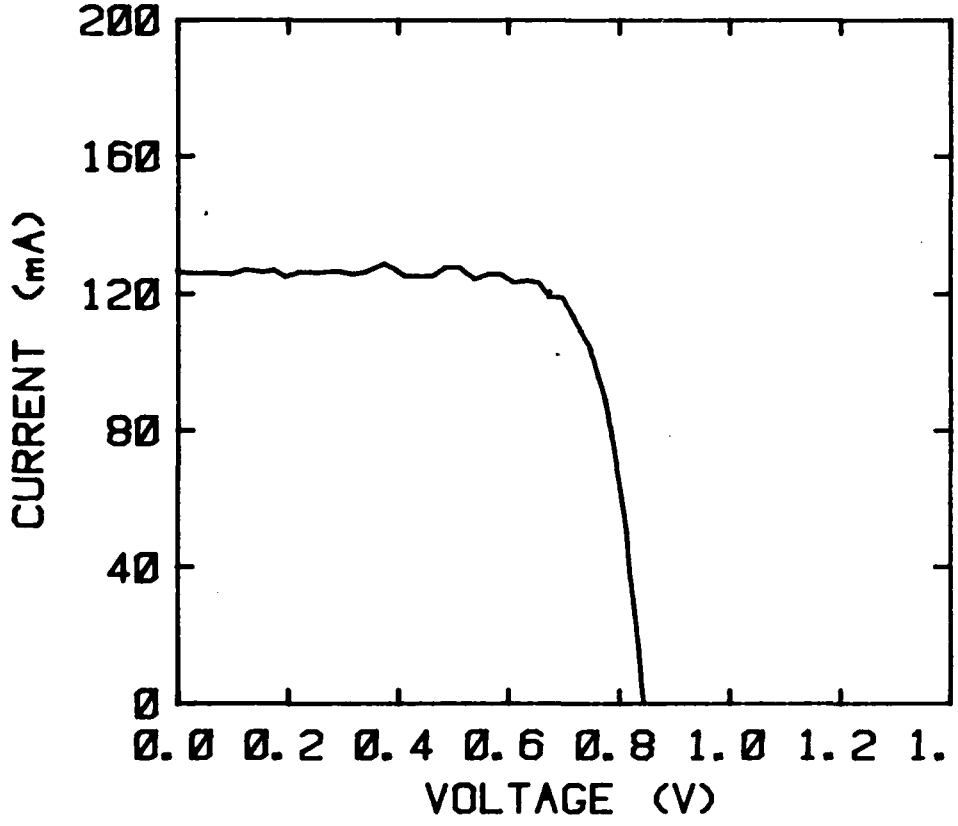

Cell 3-1-AFTER-AR		
Area	4.000	cm2
Isc	127.085	mA
Jsc	31.77	mA/cm2
Voc	0.846	V
Pmax	81.505	mW
FF	75.78	%
Eff	14.85	%
Jsc1	31.77	mA/cm2
Suns	1.0	
Vm	0.676	V
Im	120.574	mA

11-16-1989 15:52:55

Lot: 5281 Contract: 10120
Material: InP AR Coat: None
Surface: Specular Temp: 25C
Ref. Cell: ST17 Ref Isc: 8.1 mA
Comment: BEFORE FRONT CONTACT SINTER
Spectrum: AM0 (137.2 mW/cm2)
V Chan.: 3 I Chan.: 4 Cell Type: Sm. n/p

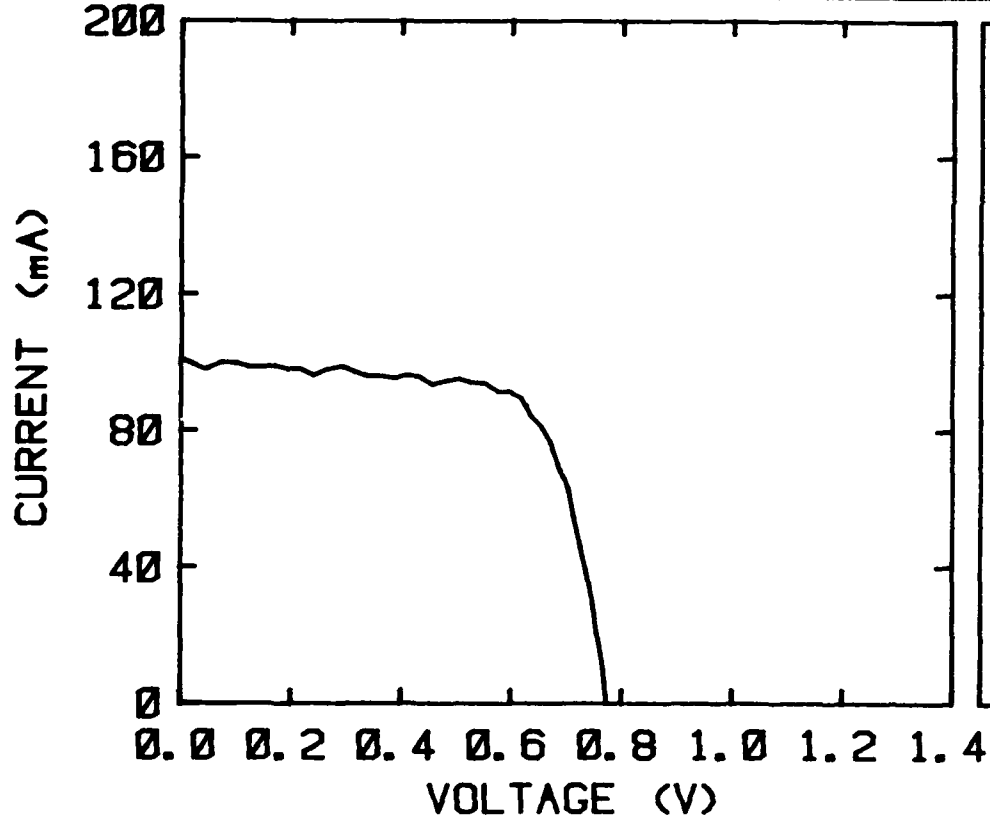

Cell	8-1-AFTER-AR	
Area	4.000	cm2
Isc	100.267	mA
Jsc	25.07	mA/cm2
Voc	0.776	V
Pmax	54.681	mW
FF	70.27	%
Eff	9.96	%
Jsc1	25.07	mA/cm2
Suns	1.0	
Vm	0.628	V
Im	87.039	mA

11-16-1989 15:50:19

Lot: 5271
Material: InP
Surface: Specular
Ref. Cell: ST17
Comment:
Spectrum: AM0 (137.2 mW/cm2)
V Chan.: 3
I Chan.: 4

Contract: 10120
AR Coat: None
Temp: 25C
Ref Isc: 8.1 mA
Cell Type: Sm. n/p

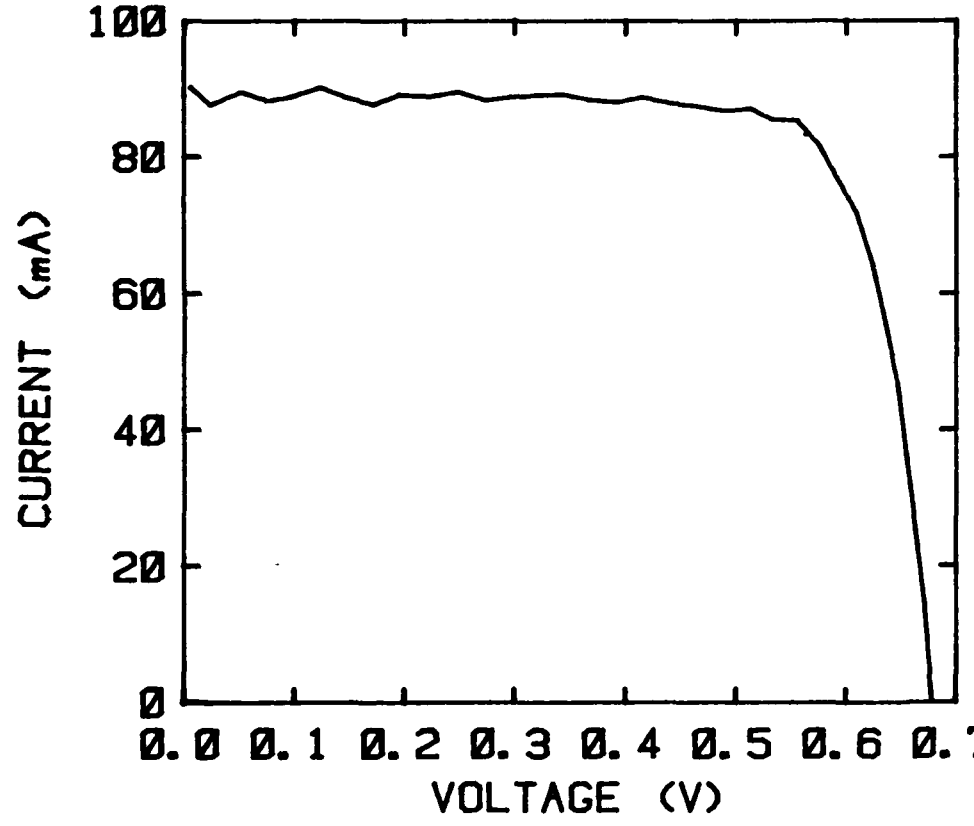

Cell 1-2		
Area	4.000	cm2
Isc	89.067	mA
Jsc	22.27	mA/cm2
Voc	0.679	V
Pmax	47.060	mW
FF	77.78	%
Eff	8.58	%
Jsc1	22.27	mA/cm2
Suns	1.0	
Vm	0.564	V
Im	83.366	mA

11-16-1989 13:35:37

Lot: 5271
Material: InP
Surface: Specular
Ref. Cell: ST17
Comment:
Spectrum: AM0 (137.2 mW/cm2)
V Chan.: 3
I Chan.: 4

Contract: 10120
AR Coat: None
Temp: 25C
Ref Isc: 8.1 mA
Cell Type: Sm. n/p

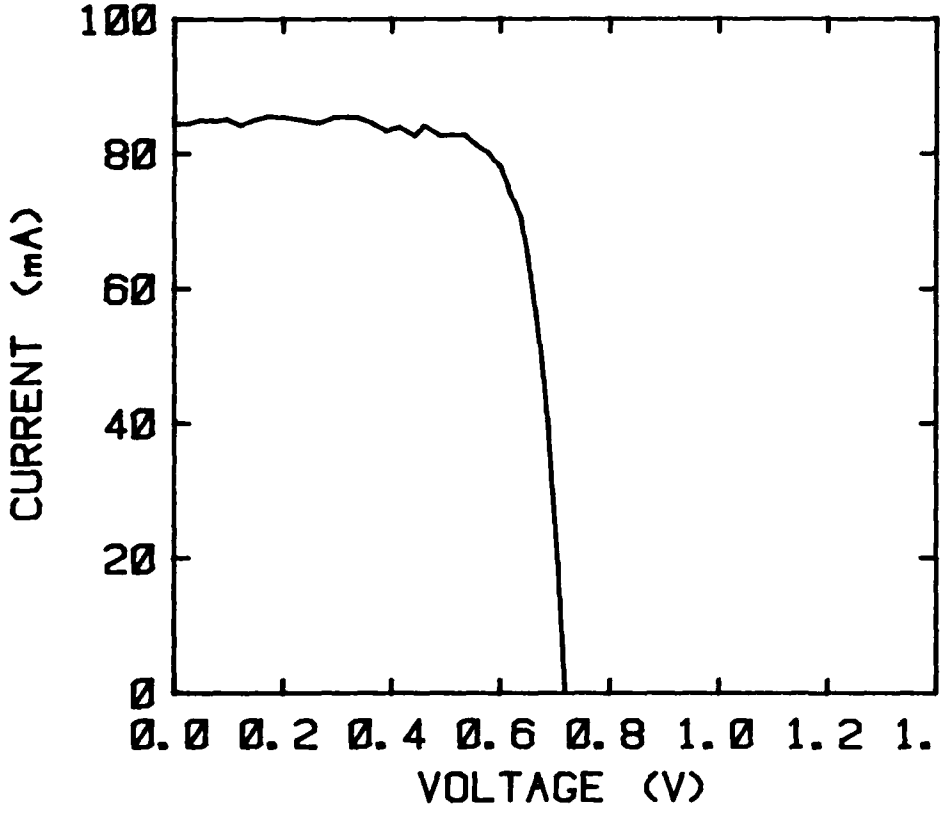

Cell 4-2		
Area	4.000	cm2
Isc	85.293	mA
Jsc	21.32	mA/cm2
Voc	0.720	V
Pmax	46.724	mW
FF	76.03	%
Eff	8.51	%
Jsc1	21.32	mA/cm2
Suns	1.0	
Vm	0.598	V
Im	78.196	mA

11-16-1989 13:31:37

Lot: 5271
Material: InP
Surface: Specular
Ref. Cell: ST17
Comment:
Spectrum: AM0 (137.2 mW/cm2)
V Chan.: 3
I Chan.: 4

Contract: 10120
AR Coat: None
Temp: 25C
Ref Isc: 8.1 mA
Cell Type: Sm. n/p

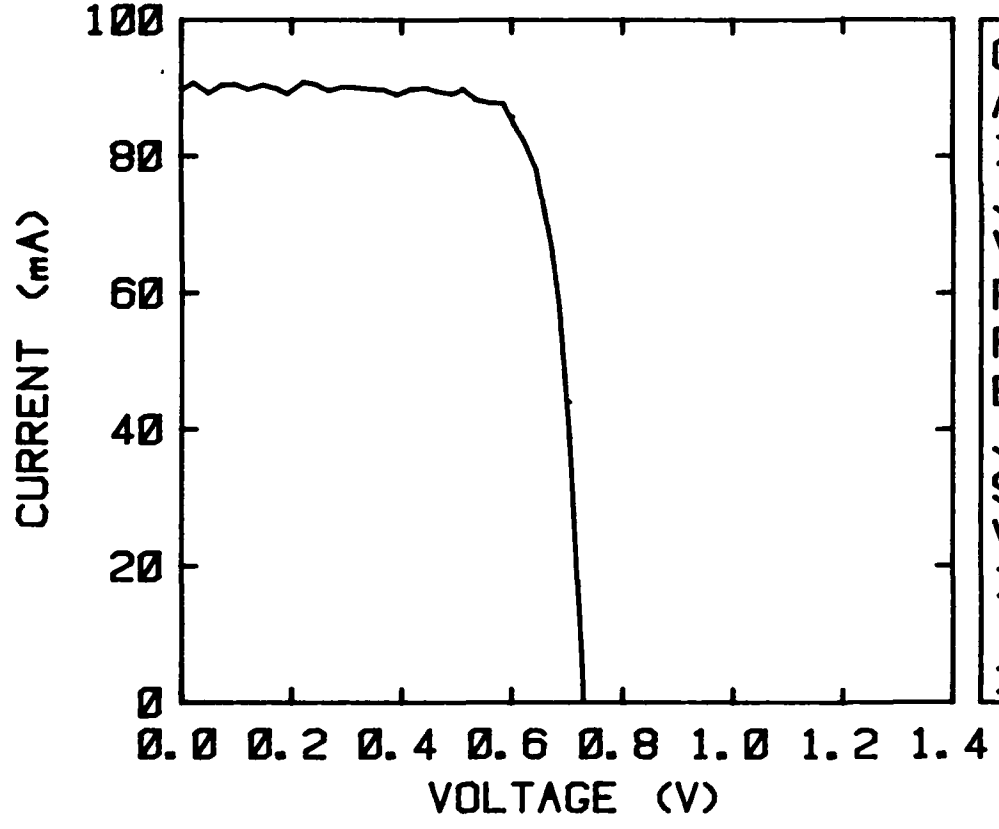

Cell 6-2		
Area	4.000	cm2
Isc	90.174	mA
Jsc	22.54	mA/cm2
Voc	0.731	V
Pmax	51.565	mW
FF	78.23	%
Eff	9.40	%
Jsc1	22.54	mA/cm2
Suns	1.0	
Vm	0.601	V
Im	85.769	mA

11-16-1989 13:46:08

Lot: 5271	Contract: 10120
Material: InP	AR Coat: None
Surface: Specular	Temp: 25C
Ref. Cell: ST17	Ref Isc: 8.1 mA
Comment:	
Spectrum: AM0 (137.2 mW/cm2)	
V Chan.: 3 I Chan.: 4	Cell Type: Sm. n/p

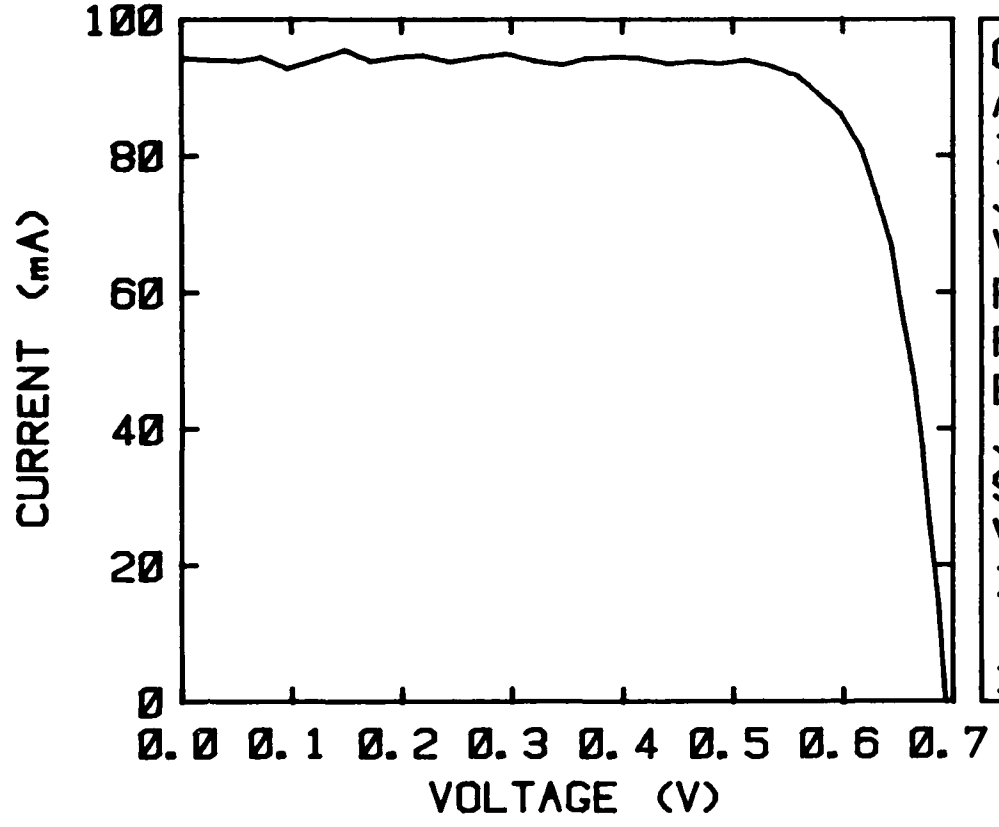

Cell 7-1		
Area	4.000	cm2
Isc	94.320	mA
Jsc	23.58	mA/cm2
Voc	0.694	V
Pmax	51.648	mW
FF	78.86	%
Eff	9.41	%
Jsc1	23.58	mA/cm2
Suns	1.0	
Vm	0.588	V
Im	87.882	mA

11-16-1989 13:39:40